SAND2011-8344C

Testing and Analysis of Low Cost Composite Materials Under Spectrum Loading and High Cycle Fatigue Conditions

John F. Mandell[1], Daniel D. Samborsky[1], Neil K. Wahl[2], and Herbert J. Sutherland[3]

[1]Montana State University, Bozeman, MT
[2]Montana Tech of the University of Montana, Butte, MT
[3]Sandia National Laboratories, Albuquerque, NM

SUMMARY: This paper provides an overview of the results of a twelve-year experimental study of low-cost composite materials for wind turbine blades. Wind turbines are subjected to 10^9 or more potentially damaging fatigue cycles over a typical service lifetime of 30 years. Stress conditions cover the range from tension dominated to compression dominated, with associated differences in and potential interactions between failure modes. Wind turbine design codes typically assume a Miner's rule linear damage law to predict failure from constant amplitude test data, which appears to be significantly non-conservative. The paper summarizes results from three areas. First, an extensive constant amplitude database including over 8800 test results with varying R-value (minimum stress / maximum stress) on over 150 materials, including variations in type of fiber and matrix, fiber content, reinforcement architecture, environment, flaws, and manufacturing method. Second, for a single E-glass/polyester material system, a study of spectrum loading effects. The third area is a study of high cycle fatigue behavior, including some specialized tests to 10^{10} cycles.

New results are presented comparing typical wind turbine loads from a long term study, resolved by R-ratio, with a detailed data set for a typical structural laminate, tested at thirteen R-values. These results allow a direct comparison of turbine loads and material fatigue resistance at each R-ratio. The Goodman diagram is the most detailed to date, including several loading conditions which have been poorly represented in earlier studies. The new data should allow more accurate lifetime prediction under spectrum loading.

KEYWORDS: Fiberglass, Fatigue, High Cycle, Spectrum Loads, Wind Turbine Blades

INTRODUCTION

Most turbine blades are constructed from low cost forms of composite materials, with manufacturing primarily by wet hand lay-up or resin infusion using woven or stitched E-glass fabric architectures. Some blades also use relatively low cost, low cure temperature forms of prepreg. While finished blade costs are on the order of $10/Kg, the performance required of blades is impressive, with higher levels of fatigue loading than for most fixed wing or rotary aircraft blades [1]. As wind turbines expand in both size and importance, improvements in materials and lifetime prediction methodologies are essential. This paper presents an overview of over a decade of research on blade materials. New results are also presented for fatigue loading for a typical blade in service, resolved by R-value, and corresponding fatigue test data for a typical laminate at the same R-values. Reviews of blade loadings and material response maybe found in References 1 - 5. References 1 - 3, as well as most of the remaining papers cited are available through the Sandia National Laboratories website: www.sandia.gov/Renewable_Energy/wind_energy/topical.htm.

A TYPICAL TURBINE BLADE LOADING SPECTRUM

The importance of correctly and completely representing the material response over a broad range of loading conditions is best illustrated by examining the loads spectrum on an operating wind turbine. In a recent measurement campaign, Sutherland et al [6, 7] obtained a long-term database for an operating turbine. This program, called the Long term Inflow and Structural Test (LIST) program, obtained inflow and structural data on a three-bladed, upwind wind turbine that is being tested at a site that is representative of most Great Plains commercial sites. Only a short description of the turbine is provided here. Sutherland [6] provides a complete discussion of the turbine and the measurement campaign.

The LIST turbine, see Figure 1, is a Micon 65/13M. It is a fixed-pitch turbine with a 3-phase 480V asynchronous generator rated at 115kW. The generator operates at 1200 rpm while the blades turn at a fixed 55-rpm. The turbine is fitted with Phoenix 8m blades that are based on Solar Energy Research Institute (SERI is now the National Renewable Energy Laboratory, NREL) airfoils. These "SERI" blades are 7.9 m (312 in) long and are equipped with tip brakes.

Typically, the fatigue spectra for the two primary blade-bending moments (edge and flap) are presented as 3-D plots of the cycle count versus cyclic amplitude and cyclic mean, see Figure 2. Figure 2a illustrates the fatigue spectrum for edge-bending and Figure 2b illustrates the fatigue spectrum for flap-bending. These spectra are typical of the fatigue spectra that one would expect for this class of turbines. Namely, the edge-bending spectra display a bi-modal distribution that is directly attributed to the large one per revolution component of the bending moment created by the rotating blade. The flap-bending moment has a very different character, with a single-mode distribution.

Unfortunately, while these plots completely describe the fatigue load spectrum, they do not readily provide an insight into where the cycles fit into a Goodman diagram. This diagram is typically used in blade design, and it represents each cycle in terms of mean and alternating stresses [1]. To provide this insight, the data from the LIST turbine were reprocessed to determine the root edge and flap strains. In this process, the amplitude of the bending strain and the total mean strain (the total mean strain is obtained by adding the rotating-blade component of strain to the mean strain for each fatigue cycle) were used to determine the appropriate R-value for each cycle. The cycles were then binned by R-value. Samples of these data are shown in Figures. 3-6. The first two plots are for the "tension" side of the bending moment (i.e., a positive bending moment produces a tensile load in the outer fibers of the root), and the second two are for the "compressive" side. In all four plots, the distributions are plotted on a Goodman diagram grid, described in more detail later. The vertical axis is the amplitude of the fatigue cycle and horizontal axis in the mean of the fatigue cycle. To the right of the vertical axis is a tensile mean and to the left is a compressive mean. The distributions of cycles are plotted along their respective constant R-value lines. For clarity in the presentation, the axes are not labeled. In all of the plots, the scale for the number of cycles is logarithmic. Actual stresses and cycle counts would depend on local stress concentrations and length of service, respectively.

Taken together, the plots show significant cycles over most of the potential loading conditions. These will be compared later with typical material response along the radial lines that represent constant values of the stress ratio R, the ratio of minimum to maximum stress or strain.

Figure 1. The List Turbine, near Bushland, Texas

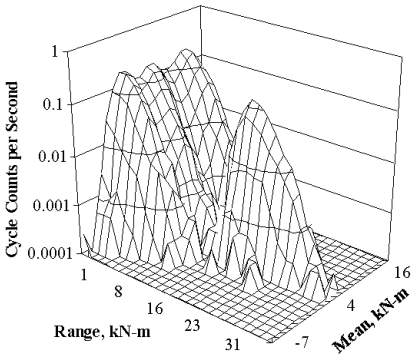

2a. Root Edge-Bending

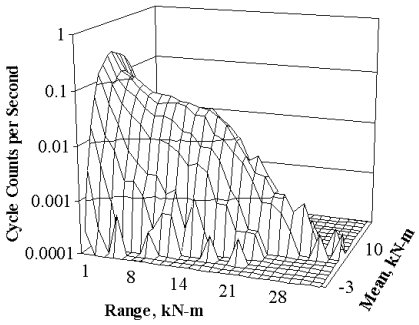

2b. Root Flap-Bending

Figure 2. Fatigue Load Spectrum for 1-Hour in the 15-to-17 m/s Wind Speed Bin.

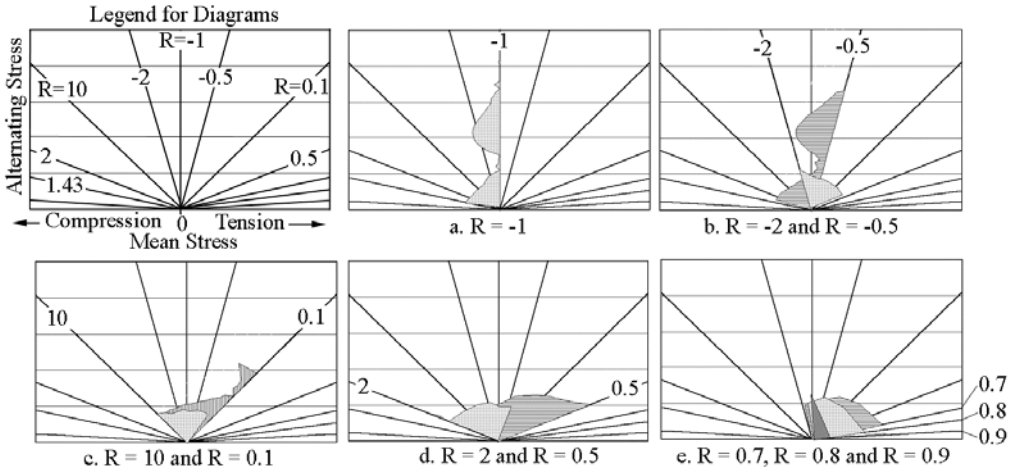

Figure 3. Fatigue Cycles for Edgewise Strains by R Value on the Tension Bending Side of the Blade. Cycle counts have a logarithmic scale; 9 to 11 m/s Wind Speed Bin.

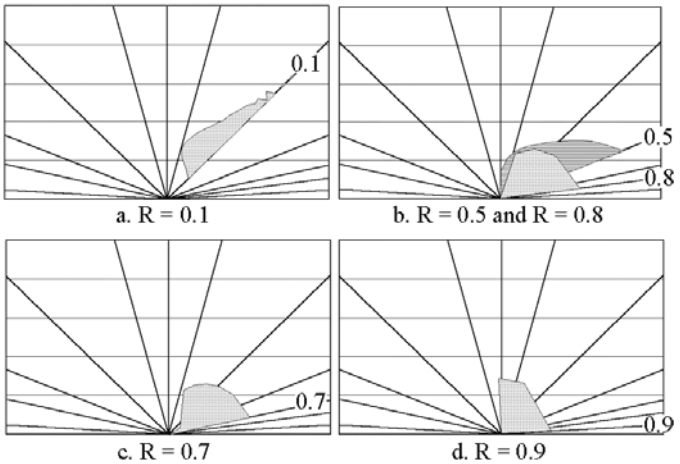

Figure 4. Fatigue Cycles for Flapwise Strains by R Value on the Tension Bending Side of the Blade. Cycle counts have a logarithmic scale; 9 to 11 m/s Wind Speed Bin.

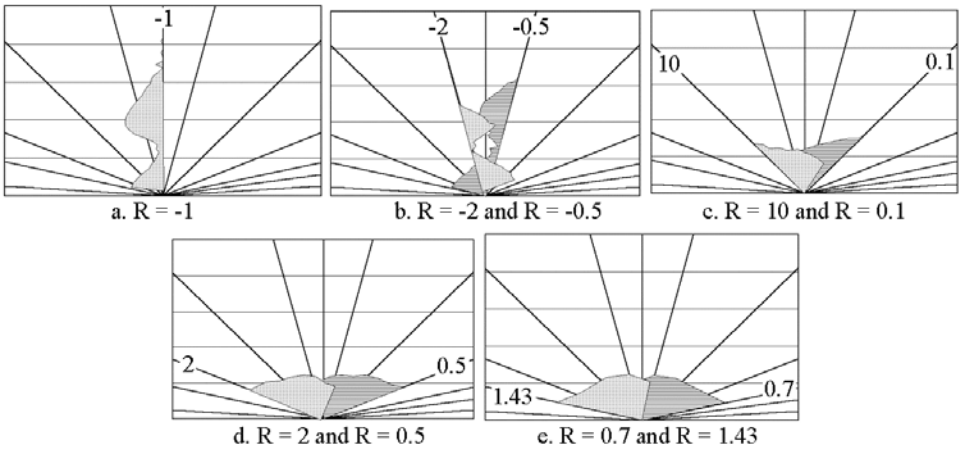

Figure 5. Fatigue Cycles for Edgewise Strains by R Value on the Compression Bending Side of the Blade. Cycle counts have a logarithmic scale; 9 to 11 m/s Wind Speed Bin.

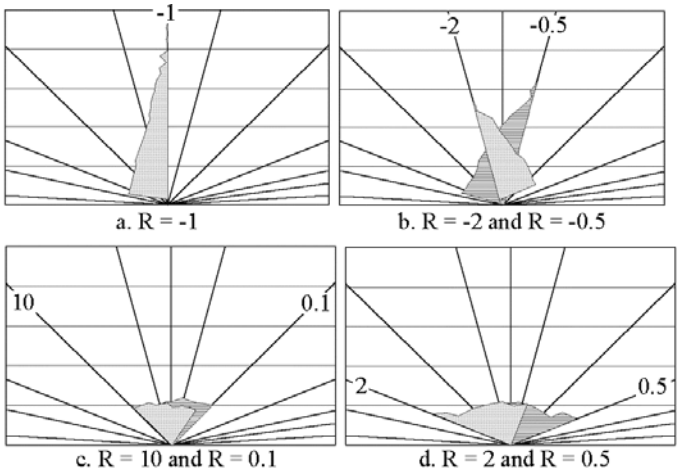

Figure 6. Fatigue Cycles for Flapwise Strains by R Value on the Tension Compression Side of the Blade. Cycle counts have a logarithmic scale;9 to 11 m/s Wind Speed Bin.

FATIGUE RESPONSE OF TYPICAL LAMINATES

Overview of Fatigue Database

The DOE/MSU fatigue database contains over 8800 test results for over 130 material systems. It is available to the public on the Sandia website given earlier. References 2 and 3 provide a detailed analysis of data trends and blade substructure applications; substructure applications are also addressed in Reference 8.

Most composite blades have been constructed from low cost forms of E-glass fabrics, with various polyester, vinyl ester, and epoxy resins. As blades have become larger, now approaching the 60 m range, a potential switch to low cost forms of carbon fibers and hybrids is under consideration [9 - 11]. While the various forms of E-glass laminates are most sensitive to tensile fatigue [2, 3], the low cost carbon fiber laminates appear limited by compression, particularly for processes with poor control of fiber alignment. Blade substructures may also fail by delamination, which has been explored in detail in recent years for various relatively low cost resins and environmental conditions [3, 12]. The database also contains results

for static and fatigue response under a range of temperature and moisture conditions [3, 13]; as usual for polymer composites, hot/wet conditions are most limiting, with ortho-polyester resins performing poorly.

Most notable in terms of fatigue resistance are the effects of fiber content and fabric architecture. Typical blade processes produce fiber contents ranging from V_F = 0.30 to 0.40 for hand lay-up, 0.45 to 0.50 for infusion and bag methods and about 0.50 for prepregs. Typical results for the tensile fatigue resistance, represented by the maximum strain to produce failure at 10^6 cycles under constant amplitude loading, are given in Figure 7. These resin transfer molded laminates contain a stitched fabric with relatively straight, tight strands, D155, for the 0° plies, and a stitched ±45° fabric DB120 in the ply configuration $[0/\pm45/0]_S$. This lay-up, typical of the primary blade structure in turbine blades, is about 70% 0° material. The transition to a much lower strain capability as the fiber content increases above 0.40 is found with all glass fabrics having discrete strands [2, 3]. Fabrics having architectures which tightly stitch various layers together, such as triaxial fabrics, produce poor tensile fatigue resistance even at very low fiber contents, below 0.30 [2, 3]. The fiber content effect illustrated in Figure 7 has been related to local pinching of strands, producing very high local fiber contents at stitch or weave points. Architectures like typical prepreg, with well-dispersed fibers, show decreased tensile fatigue strains only at fiber contents above 0.60.

The second notable trend in the database relates to compressive static strength. As is well known in the advanced composite industry, even small amounts of fiber misalignment can produce significant decreases in compressive strength. The weave geometry in typical woven fabric laminates often produces a loss in strength of the order of 50%, compared to composites with straight fibers. Low cost composites are typically more heterogeneous than prepreg, and this often produces fiber waviness. Even when fiber strands are stitched onto other layers like mat, the waviness around the stitching produces major compressive strength reductions [3, 9, 10]. The waviness issue is particularly important with low cost carbon fiber forms, where the baseline ultimate strains for relatively straight fibers are only about half of the corresponding values for glass fiber laminates. In addition to fiber waviness present in fabrics, severe waviness can be introduced by fiber wash in resin infusion processes, and by the distortion of plies near structural details like ply drops [3, 9, 10].

Spectrum Loading Effects

Most of the fatigue results in the database are for constant amplitude loading at particular R-values. These must be assembled into an overall Goodman diagram representation (shown later) covering all values of mean stress and stress amplitude, which can then be used with an appropriate cumulative damage law, like Miner's sum (Equation 1), to predict the lifetime of the material for a particular load spectrum.

$$Miner's\ Sum = D = \sum_i \frac{n_i}{N_i} \tag{1}$$

where D at failure is usually taken as 1.0, n_i is the number of cycles at stress level S_i, and N_i is the number of cycles to failure at S_i. Efforts to predict test coupon lifetimes under spectrum loading have produced disappointing results [3, 14, 15]. Data are typically obtained from tests where the maximum load in the spectrum is varied, with the spectrum repeated until failure, for different maximum loads. Figure 8 shows typical results from Reference 14, where the spectrum used is a standardized European WISPERX wind turbine fatigue load spectrum [16]. Regardless of the cumulative damage law used, Miner's sum or linear or nonlinear residual strength (NRSD), the lifetime predicted from a Goodman diagram constructed from five R-values over-predicts the lifetime by about an order of magnitude. This has been found for most, but not all fiberglass materials [14, 15, 17].

Reference 14, from which Figure 8 was taken, reports on a detailed study of spectrum loading effects using a typical laminate from the database, material DD16. This laminate has the configuration $[90/0/\pm45/0]_S$, with a fiber volume fraction of 0.36, typical of hand layed-up blades. The 90° and 0° plies are D155 stitched unidirectional fabric, the ±45° plies are DB120 stitched fabric, and the resin is an ortho-polyester. Test methodologies are described in detail in Reference 14. A series of tests using simple two-load blocks of different durations and loads, repeated to failure, showed results like Figure 9. When the blocks were not completely dominated by one stress level, the lifetime fell short of the Miner's sum prediction, and was best predicted by a nonlinear residual strength theory. (An NRSD model using both exponential and power law fits to the constant amplitude test data are shown.) However, the more complex spectrum used for Figure 8 resulted in non-conservative lifetime predictions for all cumulative damage theories explored, as noted above.

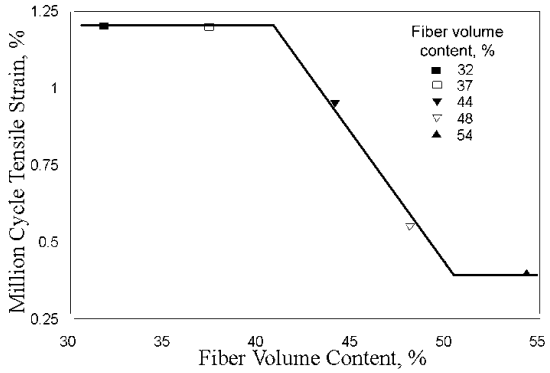

Figure 7. Million Cycle Tensile Fatigue Maximum Strain versus Fiber Content for $[0/\pm45/0]_S$ Laminates, R=0.1.

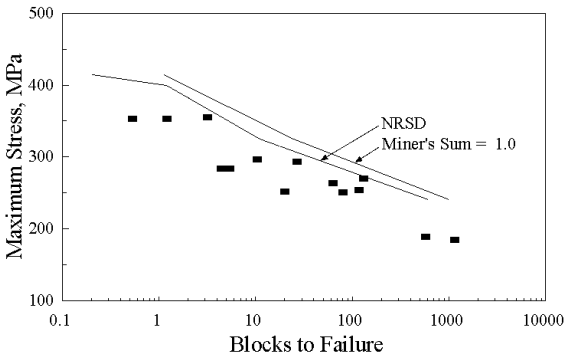

Figure 8. Lifetime Data for WISPERX Spectrum versus Prediction based on Miner's Sum and NRSD Models.

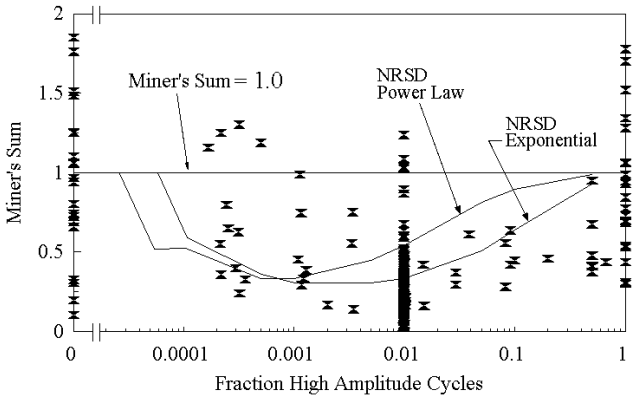

Figure 9. Lifetime Data in Terms of Miner's Sum at Failure with Predictions for Two-Block Spectrum at 325/207 MPa Maximum Stress Levels (R=0.1); Exponential and Power Law Fatigue Models With Nonlinear Residual Strength Cumulative Damage Law (NRSD), Compared with Miner's Sum = 1.0.

Goodman Diagram

Recent efforts to improve the accuracy of spectrum loading lifetime predictions have led to the development of a more complete Goodman diagram than previously available, and a more accurate fatigue model (Equation 2). Figure 10 provides constant amplitude data for thirteen R-values. The constant load tension (R=1) data are plotted by assuming a frequency of 10 cycles/second, typical of the cyclic tests. Many of the R-values produced semi-log stress versus log cycles S-N trends with complex

shapes, relatively flat at low cycles, steeper at medium cycles, and less steep again at high cycles. It was found that at least three parameters were needed to fit these trends. Several such models are available in the literature [18, 19]. The particular model used here is a variation of that in Reference 19

$$S_O - S = aS\left[\frac{S}{S_O}\right]^b (N^c - 1) \tag{2}$$

where S is the maximum applied stress, S_O is the ultimate tensile or compressive strength (obtained at a strain rate similar to the 10 Hz fatigue tests), and a, b, and c are the fitting parameters. Additionally, the maximum stress value extrapolated to 10^9 cycles was kept within 10% of the extrapolated stress from a power law fit to the data for cycles above 10^3,

$$\frac{S}{S_O} = AN^B \qquad \text{Fit to cycles} > 10^3 \tag{3}$$

Table 1 provides the constants used to fit each R-value using Equation (2), as well as the power law high cycle curve fit parameters, A and B, for Equation (3).

Forcing of the high-cycle extrapolations to fit Equation (3) is based on literature data trends at high cycles for fiberglass composites [18, 20] and on recent results obtained at very high cycles for small strands [3, 21]. The small strand data at R=0.1 are fit well by Equation (3) out to 10^{10} cycles, as shown in Figure 11. The small strand data trends agree well with larger strand data that are available to 10^8 to 10^9 cycles, and standard laminate data out to 10^7 to 10^8 cycles. (However, the absolute stress and strain levels for the small strands are significantly higher than for typical laminates [3, 21].) The other common fatigue model used to fit S-N data, the exponential model (Equation 4) provides a poor fit at high cycles

$$\frac{S}{S_O} = A - bLogN \tag{4}$$

where A and b are constants.

The data trends shown in Figure 10, using Equation (2), were used to construct the Goodman diagram in Figure 12, where constant R-value S-N curves plot along radial lines. The new data refine the earlier Goodman diagrams [3, 14, 15] for R-values involving reversed loading, -2, -1 and –0.5, as well as high tensile R-values, 0.7 to 1.0. The high tensile R-value data, in particular, produce a much more conservative Goodman diagram in this range, which may improve spectrum loading predictions [9].

Comparison of Figures 3 – 6 with Figure 12 provides a visual impression of the types of loading which will be most damaging for this particular material. Unfortunately, most loading conditions appear capable of producing significant damage. The higher cycle tensile fatigue domain appears particularly sensitive. Other materials (such as carbon fiber) and other turbine designs and wind conditions may produce different areas of sensitivity. In future work, these data will be used in predicting damage contributions and in comparing fatigue design methodologies. The Goodman diagram data set also provides an improved basis for defining fatigue data requirements for materials of interest for blades. For this material, testing at R-values of 1.0, 0.7, -1 and possibly -2 would allow construction of a diagram with a reasonable compromise of data requirements and accuracy, with generally conservative approximations. The important R=1.0 trend might be common to most laminates if normalized by a typical static strength test [3].

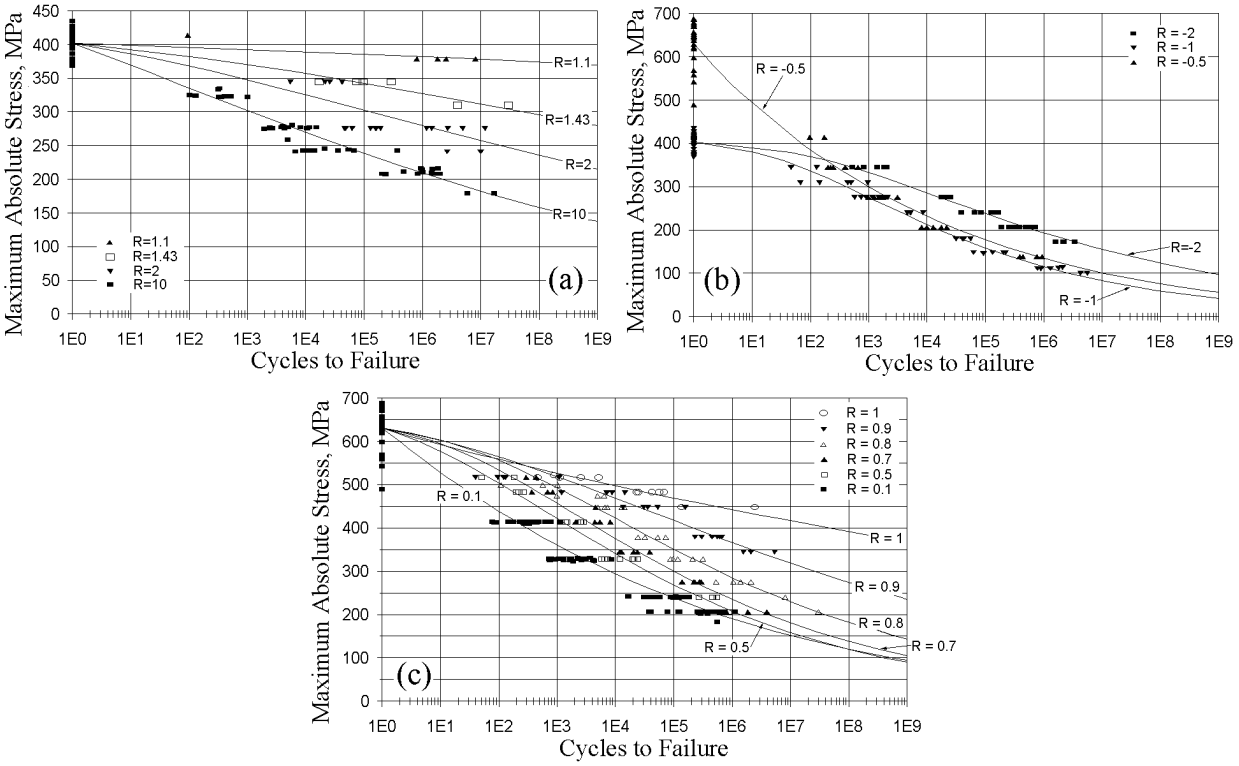

Figure 10. Maximum Absolute Stress versus Cycles to Failure for Thirteen R-Values for Database Material DD16, Fit with Equation 2.

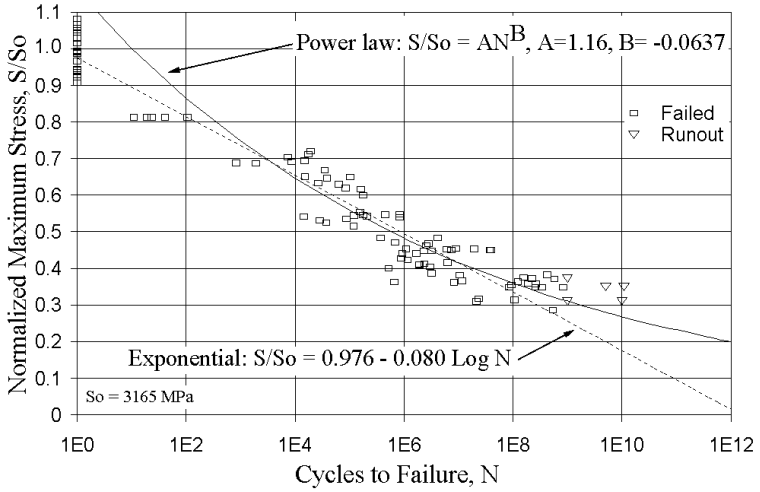

Figure 11. Normalized Tensile Stress versus Log Cycles for Small Strands, with Power Law and Exponential Trend Lines.

CONCLUSIONS

The effects of a broad range of material parameters and loading conditions on the fatigue of low cost laminates are available in the DOE/MSU database. The application of constant amplitude fatigue data to predict lifetime under spectrum loading has been problematical. New data allow construction of a more detailed Goodman diagram which may improve spectrum loading predictions and identify minimum

fatigue data requirements. Actual spectrum loads from service conditions provide more meaningful information when resolved to different R-value ranges, for comparison to the Goodman diagram.

Table 1. Equation 2 and 3 Parameters for the Thirteen R-Values for Material DD16 and for Small Strands.

R - Value	Model (Equation 2)			Power Law (Equation 3)	
	a	b	c	A	B
1.1	0.060	3.0	0.05	402.2	-0.0038
1.43	0.060	3.0	0.15	401.8	-0.0148
2	0.060	4.0	0.25	458.2	-0.0372
10	0.100	4.0	0.35	391.3	-0.0445
-2	0.010	4.0	0.55	648.4	-0.0876
-1	0.020	3.0	0.62	716.8	-0.1317
-0.5	0.450	0.85	0.25	621.8	-0.1134
0.1	0.420	0.58	0.18	629.5	-0.0865
0.5	0.075	2.5	0.43	832.5	-0.0997
0.7	0.04	2.5	0.45	995.6	-0.1059
0.8	0.035	2.5	0.40	1007	-0.0924
0.9	0.060	2.5	0.28	811.0	-0.0574
1*	0.21	3.0	0.14	598.5	-0.0205
Small Strand	0.25	3.7	0.3	1.053	-0.0561

*Assumes a frequency of 10 Hz.

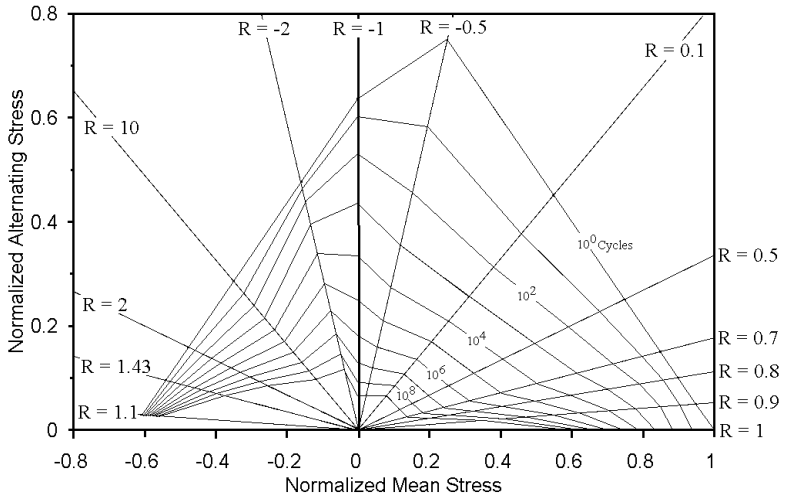

Figure 12. Goodman Diagram for Database Material DD16.

ACKNOWLEDGEMENTS

The studies at Montana State University are carried out under subcontracts from Sandia National Laboratories; Sandia is a multi-program laboratory operated by Sandia Corporation, a Lockheed Martin Company, for the US Departmental of Energy under Contract DE-AC04-94AL85000.

REFERENCES

1. H.J. Sutherland, “On the Fatigue Analysis of Wind Turbines,” Report SAND99-089, Sandia National Laboratories, Albuquerque, NM (1998)

2. J.F. Mandell, and D.D. Samborsky, "DOE/MSU Composite Material Fatigue Database: Test Methods, Materials, and Analysis," Report SAND97-3002, Sandia National Laboratories, Albuquerque, NM (1997).
3. J.F. Mandell, D.D. Samborsky, and D.S. Cairns, "Fatigue of Composite Materials and Substructures for Wind Turbine Blade," Contractor Report SAND2002-077, Sandia National Laboratories, Albuquerque, NM (2002).
4. R.M. Mayer, "Design of Composite Structures Against Fatigue," Mechanical Engineering Publications Ltd., Suffolk, G.B. (1996).
5. H.J. Sutherland, Wind Energy, 3, 2000, pp. 1-34.
6. Sutherland, H.J., P.L. Jones, and B. Neal, 2001, Proc. 2001 ASME Wind Energy Symposium, ASME/AIAA, New York, 2001, pp. 1-12.
7. Sutherland, H.J., Solar Energy Engineering, Trans. ASME, v.124, 2002, pp. 432-445.
8. J.F. Mandell, D.D. Samborsky, D.W. Combs, M.E. Scott and D.S. Cairns, "Fatigue of Composite Material Beam Elements Representative of Wind Turbine Blade Substructure," Report NREL/SR-500-24374, National Renewable Energy Laboratory, Golden, Co (1998).
9. J.F. Mandell, D.D. Samborsky, L. Wang, and N.K. Wahl, in Proc. 2003 ASME Wind Energy Symposium, ASME/AIAA, New York (2003), pp. 167-179.
10. J.F. Mandell, D.D. Samborsky, and L. Wang, "Effects of Fiber Waviness on Composites for Wind Turbine Blades," Proc. SAMPE 2003, Society for the Advancement of Materials and Process Engineering, Corina, Ca (in press).
11. D.A. Griffin and T.D. Ashwill, Proc. 2003 ASME Wind Energy Symposium, ASME/AIAA, New York, 2003, pp. 191-201.
12. J.F. Mandell, D.S. Cairns, D.D. Samborsky, R.B. Morehead, and D.H. Haugen, Proc. 2003 ASME Wind Energy Symposium, ASME/AIAA, New York, 2003, pp. 200-213.
13. J.F. Mandell, D.D. Samborsky, M. Li., R. Orozco, and D.S. Cairns, Proc. of the 2000 ASME Wind Energy Symposium, ASME/AIAA, New York, 2000, pp. 354-366.
14. N.K. Wahl, J.F. Mandell, D.D. Samborsky, "Spectrum Fatigue Lifetime and Residual Strength for Fiberglass Laminates," Report SAND2002-0546, Sandia National Laboratories, Albuquerque, NM (2002).
15. R.P.L. Nijssen, D.R.V. van Delft, A.M. van Wingerde, in Proc. 2002 ASME Wind Energy Symposium, ASME/AIAA, New York, 2002, pp.10-18.
16. A.A. ten Have, "WISPER and WISPERX, Final Definition of Two Standardizd Fatigue Loading Sequences for Wind Turbine Blades," NRL TP91476U, National Aerospace Laboratory NRL, The Netherlands, (1992).
17. A.T. Echtermeyer, C. Kensche, P. Bach, M. Poppen, H. Lilholt, S.I. Andersen, and P. Brøndsted, Proc. of 1996 European Union Wind Energy Conference (1996).
18. G.P. Sendecky, in "Fatigue of Composite Materials," K.L. Reifsnider, ed., Elsevier, The Netherlands, 1991, pp. 431-483.
19. J.A. Epaarachchi and P.D. Clausen, "A Model for Fatigue Behavior Prediction of Glass Fibre Reinforced Plastic Composites for Various Stress Ratios and Test Frequencies" (in press)
20. D.R.V van Delft, G.D. de Winkle, and P.A. Josse, 1997 ASME Wind Energy Symposium, AIAA/ASME, New York, W. Musial and D.E. Berg, eds., 1997, pp. 180-188.
21. D.D. Samborsky, and J.F. Mandell, "Very High Cycle Tension Fatigue of Impregnated E-glass Strands" (in press).